SPE 106179

Multiscale Mixed Finite Element Modeling of Coupled Wellbore/Near-Well Flow

S. Krogstad, SINTEF ICT, and L. J. Durlofsky, SPE, Stanford University

This paper was prepared for presentation at the 2007 SPE Reservoir Simulation Symposium held in Houston, Texas, U.S.A., 26–28 February 2007.

Abstract

An accurate well modeling capability is important for both production and reservoir engineering calculations. Ideally, the models used for these two applications should be related in a logical manner. Multiscale methods allow varying degrees of resolution and can therefore provide a natural linkage between production and reservoir models. In this work, we present a coupled wellbore-reservoir flow model that is based on a multiscale mixed finite element formulation for reservoir flow linked to a drift-flux wellbore flow representation. The model is able to capture efficiently the effects of near-well heterogeneity in the reservoir and phase holdup and pressure variation in the wellbore. The formulation presented here is for oil-water systems. The basic reservoir-wellbore linkage is described and validated through comparison to results from an existing simulator. The multiscale methodology is then applied to a heterogeneous reservoir model. Both vertical and deviated wells are considered. Comparisons of the multiscale solution to the fully resolved (fine-scale) solution demonstrate the high degree of accuracy of the method, for both reservoir and wellbore quantities, as well as its efficiency.

Introduction

The accurate modeling of near-well flow effects is essential for large-scale reservoir simulation and detailed production engineering calculations. Near-well models should ideally include wellbore and reservoir flow effects and should be suitable both as standalone well production applications and as modules in reservoir simulators. Multiscale finite element methods are in concept well-suited for this type of modeling, as they allow varying resolution and provide a systematic procedure for coarsening and refining. Thus they can provide the basis for a modeling framework that maintains consistency between reservoir and production engineering models. To our knowledge, however, multiscale methods have not yet been applied for this problem.

In this work, we develop a multiscale mixed finite element method (MsMFEM) for modeling coupled wellbore and near-well flow. The MsMFEM solves the pressure equation (in the reservoir domain) on a coarse grid, but captures fine-scale effects through basis functions determined from numerical solutions of local single-phase flow problems on the underlying fine-scale geological grid. We fully resolve the well trajectory on the fine scale using a flexible grid, which is close to radial around the well but logically Cartesian away from the well. The flow within the wellbore is represented using a drift-flux model. This model captures the slip between phases and provides the in-situ phase fractions (holdup), which provide a means for computing the pressure profile within the wellbore. Pressure variation within the wellbore is important in many settings as it impacts the local inflow from the reservoir into the well (in the case of a production well).

Multiscale methods for reservoir simulation have been introduced as an alternative to standard upscaling as a tool for more fully incorporating fine-scale features at low computational cost. Among the relevant approaches are the multiscale finite element methods (e.g., Hou and Wu, 1997), the multiscale finite volume method (Jenny *et al.*, 2003) and the multiscale mixed finite element method (Chen and Hou, 2003). The variational multiscale approach of Arbogast (2000), also formulated within a mixed finite element context, represents another related methodology. Here we consider a version of the multiscale mixed finite element method (MsMFEM) introduced by Aarnes (2004) and extended in later publications (Aarnes *et al.*, 2006a, 2006b). Well representations have been incorporated into multiscale formulations by, for example, Chen and Yue (2003) and Wolfsteiner *et al.* (2006), though these formulations did not include wellbore flow effects. As far as we are aware, multiscale formulations have not been applied previously to detailed near-well models that include both reservoir and wellbore flow effects.

Wellbore flow modeling within the context of reservoir simulation is often accomplished using drift-flux (or related) models. These models are well suited for use in reservoir simulation as they are simple, continuous and differentiable. The drift-flux representation (Zuber and Findlay, 1965) includes two basic parameters – the profile parameter C_0 and the drift velocity V_d. These quantities depend on system parameters such as phase flow rates, well inclination and fluid properties. The general drift-flux model applied here is based on the formulation originally introduced by Holmes (1977) and Holmes *et al.* (1998). In recent work (Shi *et al.*, 2005a), the model parameters for two-phase flow (gas-liquid and oil-

water) were optimized based on large-scale experiments involving a 15 cm diameter inclinable flow loop (see Oddie *et al*., 2003, for details of the experiments). In the current work, we apply the drift-flux model described in Shi *et al*. (2005a). We note that the model was subsequently extended to three-phase wellbore flow (Shi *et al*., 2005b), though we do not consider flows of this type here.

This paper proceeds as follows. After introducing the model equations, we briefly present three mixed finite element approximation techniques relevant for this paper: the standard Raviart-Thomas approach, mimetic finite differences, and the MsMFEM. The drift-flux model for computation of wellbore in-situ phase fractions and pressure drop is then presented, followed by a description of its coupling to the MsMFEM. Next, we validate the mimetic finite difference and MsMFEM implementations through comparison to an existing simulator. MsMFEM solutions are then compared to reference solutions for a heterogeneous model computed directly on the fine grid and close agreement is observed. We present results involving vertical and inclined wells, where slip between phases and pressure drop due to wellbore friction occur.

Numerical Procedures

Governing Equations. We consider model equations for two-phase immiscible flow in porous media. Although included in the numerical experiments of this paper, we here neglect compressibility and gravity for ease of exposition. Letting Ω denote the domain of interest, the *pressure equation* reads:

$$\begin{aligned} \mathbf{u} &= -\lambda \mathbf{k}\nabla p \quad \text{in } \Omega, \\ \nabla\cdot\mathbf{u} &= q \qquad\quad \text{in } \Omega. \end{aligned} \quad \text{.....(1)}$$

Here $\mathbf{u}$ is the Darcy velocity, p is the pressure, λ is the total mobility (which depends on water saturation S), $\mathbf{k}$ is the permeability tensor and q is the source term. We henceforth assume no-flow boundary conditions, $\mathbf{u}\cdot\mathbf{n} = \mathbf{0}$ on $\partial\Omega$, where $\mathbf{n}$ is the outward pointing unit normal. Letting the two phases be oil and water, the conservation of water is expressed via the *saturation equation:*

$$\phi\frac{\partial S}{\partial t} + \nabla\cdot(f(S)\mathbf{u}) = q_w \,. \quad \text{.....(2)}$$

Here ϕ is the rock porosity, f is the Buckley-Leverett fractional flow function, and q_w is the water source term.

Mixed Methods. The starting point for mixed finite element methods (MFEM) (Brezzi and Fortin, 1991) is the weak formulation of Eq. (1): Find $(\mathbf{u}, p) \in H_0^{\mathrm{div}}(\Omega)\times L^2(\Omega)$ such that

$$\begin{aligned} \int_\Omega \mathbf{u}\cdot(\lambda\mathbf{k})^{-1}\hat{\mathbf{u}}\,d\mathbf{x} - \int_\Omega p\nabla\cdot\hat{\mathbf{u}}\,d\mathbf{x} &= 0, \\ \int_\Omega \hat{p}\nabla\cdot\mathbf{u}\,d\mathbf{x} &= \int_\Omega q\hat{p}\,d\mathbf{x}, \end{aligned} \quad \text{.....(3)}$$

for all $(\hat{\mathbf{u}}, \hat{p}) \in H_0^{\mathrm{div}}(\Omega)\times L^2(\Omega)$. Here $L^2(\Omega)$ is the space of square integrable functions over Ω and $H_0^{\mathrm{div}}(\Omega)$ is the space of square integrable vector functions having square integrable divergence and zero flow across the boundary.

The basic idea in MFEM discretizations is to search for solutions of Eq. (3) in finite dimensional subspaces $U\times V \in H_0^{\mathrm{div}}(\Omega)\times L^2(\Omega)$. That is, find $(\mathbf{u}, p) \in U\times V$ such that Eq. (3) is satisfied for all $(\hat{\mathbf{u}}, \hat{p}) \in U\times V$. Letting $\{\boldsymbol{\psi}_k\}$ and $\{\varphi_i\}$ be bases for U and V, one obtains approximations $\mathbf{u} = \sum_k u_k\boldsymbol{\psi}_k$ and $p = \sum_i p_i\varphi_i$, where the vectors $\mathbf{U} = \{u_k\}$ and $\mathbf{P} = \{p_i\}$ solve the linear system

$$\begin{pmatrix} \mathbf{B} & \mathbf{C} \\ \mathbf{C}^T & \mathbf{O} \end{pmatrix}\begin{pmatrix} \mathbf{U} \\ -\mathbf{P} \end{pmatrix} = \begin{pmatrix} \mathbf{0} \\ \mathbf{Q} \end{pmatrix}. \quad \text{.....(4)}$$

The coefficients of the sub-matrices are given by

$$\mathbf{B}_{kl} = \int_\Omega \boldsymbol{\psi}_k\cdot(\lambda\mathbf{k})^{-1}\boldsymbol{\psi}_l d\mathbf{x}\,, \quad \text{.....(5)}$$

$$\mathbf{C}_{ki} = \int_\Omega \varphi_i\nabla\cdot\boldsymbol{\psi}_k\,d\mathbf{x} \text{ and } \mathbf{Q}_i = \int_\Omega \varphi_i q\,d\mathbf{x}\,. \quad \text{.....(6)}$$

Let $\{T_i\}$ be a collection of cells constituting a grid. Then, using the lowest-order approximation spaces, each basis function for pressure φ_i corresponds to a cell T_i, while each flux basis function corresponds to an interface (edge in 2D, face in 3D) between two neighboring cells. For two neighboring cells T_i and T_j, we henceforth denote their common interface by Γ_{ij}, and the corresponding flux basis function by $\boldsymbol{\psi}_{ij}$.

Next, we briefly describe three discretization techniques for Eq. (3): Raviart-Thomas, mimetic finite differences and MsMFEM. For all these methods the approximation space V for pressure coincides, and is simply the space of piecewise constant functions over $\{T_i\}$. So for a cell T_i, the corresponding pressure basis function φ_i is given by

$$\varphi_i(\mathbf{x}) = \begin{cases} 1/|T_i| & \text{if } \mathbf{x}\in T_i, \\ 0 & \text{otherwise.} \end{cases} \quad \text{.....(7)}$$

We now describe the approximation spaces for velocity.

Raviart-Thomas. The lowest-order classical MFEM approximation spaces are the Raviart-Thomas spaces (RT_0). For triangular/tetrahedral and regular grids, the space U is characterized by piecewise linear vector functions over $\{T_i\}$, having constant normal component across the cell interfaces. For more generally shaped grids, one usually needs mappings (Piola transforms) to reference elements to enable assembly of the linear system (4). For general grids, this is not straightforward.

Mimetic Finite Differences. Mimetic finite difference methods applied within the context of subsurface flow modeling were presented by Hyman *et al.* (1997, 2002). Although motivated by finite differences, recent versions by Brezzi *et al*. (2005a, 2005b) can be seen as a generalization of the RT_0-based method that eases treatment of more general

geometries. In particular, for two neighboring cells T_i and T_j with interface Γ_{ij}, one can define the corresponding flux basis function $\boldsymbol{\psi}_{ij}$ as the solution of the problem

$$\boldsymbol{\psi}_{ij} = -\nabla p, \quad \nabla \cdot \boldsymbol{\psi}_{ij} = \begin{cases} 1/|T_i| & \text{for } \mathbf{x} \in T_i \\ -1/|T_j| & \text{for } \mathbf{x} \in T_j \end{cases}, \quad \text{.....(8)}$$

with $\boldsymbol{\psi}_{ij} \cdot \mathbf{n} = 0$ on the boundary $\partial(T_i \cup T_j)$, and $\boldsymbol{\psi}_{ij} \cdot \mathbf{n}_{ij} = 1/\Gamma_{ij}$ on Γ_{ij}, where $\mathbf{n}_{ij}$ is the unit normal vector to Γ_{ij} pointing from T_i to T_j. For triangular/tetrahedral and regular grids, these basis functions will coincide with those in RT_0, while for general grids Eq. (8) cannot be computed exactly. However, as shown by Brezzi *et al.* (2005b), one can approximate the resulting integrals (5)-(6) solely by using boundary integrals, so there is no need to have an explicit form of the velocity inside the cells. For further details on the construction of these methods and for convergence and stability results, see Brezzi *et al.* (2005a, 2005b).

Multiscale MFEM. In the current MsMFEM (Aarnes *et al.*, 2006b) we consider two grids as in Figure 1, where the coarse grid consists of blocks containing a connected set of cells from the underlying fine grid. We let a flux basis function $\boldsymbol{\psi}_{ij}$ be a *numerical* solution of the following local problem:

$$\boldsymbol{\psi}_{ij} = -\lambda \mathbf{k} \nabla p, \ \nabla \cdot \boldsymbol{\psi}_{ij} = \begin{cases} w_i & \text{for } \mathbf{x} \in T_i \\ -w_j & \text{for } \mathbf{x} \in T_j \end{cases}, \quad \text{.....(9)}$$

with $\boldsymbol{\psi}_{ij} \cdot \mathbf{n} = 0$ on $\partial(T_i \cup T_j)$, computed on the fine grid. In (9), w_i is a weight function of unit integral over T_i. In particular, we choose

$$w_i = \begin{cases} q(\mathbf{x}) / \int_{T_i} q(\mathbf{x})\, d\mathbf{x} & \text{if } \int_{T_i} q(\mathbf{x})\, d\mathbf{x} \neq 0 \\ \text{trace}(\mathbf{k}(\mathbf{x})) / \int_{T_i} \text{trace}(\mathbf{k}(\mathbf{x}))\, d\mathbf{x} & \text{otherwise} \end{cases}. \quad (10)$$

The above choice for cells with nonzero source q over T_i ensures a conservative approximation on both the fine and coarse scales. In the case when q is zero over T_i, the weight function to some extent reflects the permeability in the block. We remark that this choice improves the overall accuracy of the method compared to using just a constant weight, even for anisotropic tensors (Aarnes *et al.*, 2006a). In principle, any conservative solver can be used for the local fine-grid problems (9), but the RT_0-MFEM and mimetic finite differences are especially well suited because they enable direct and exact evaluation of the coefficients (5)-(6) for the coarse system. In the numerical examples presented in this paper, we apply a mimetic discretization which reduces to RT_0 for regular grids and scalar permeability.

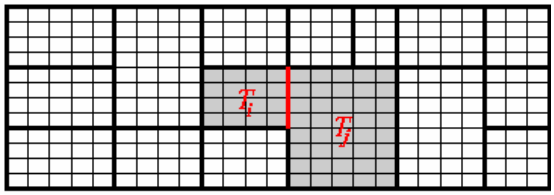

Figure 1: A fine rectangular grid partitioned into coarse blocks constituting the coarse grid.

MsMFEM for Two-phase Flow Simulations. In two-phase flow simulations, where the pressure and saturation equations (1)-(2) are solved sequentially, the MsMFEM provides computational efficiency because the computed basis functions (9) can be reused through several timesteps. As has also been noted for the multiscale finite volume method (Jenny *et al.*, 2004), at most the updating of basis functions near the front is necessary (this assumes the basis functions are computed locally as in (9) rather than globally). For moderate mobility ratios, the updating of basis functions is generally not required. It follows that the computational cost of using the MsMFEM is comparable to that of a flow-based upscaling method. Thus, the use of MsMFEM for two-phase flow simulation can be described by the following steps:

Initially compute basis functions corresponding to coarse interfaces.
for $n = 1$ **to** N
- If desired, update basis functions in blocks having steep saturation gradients
- Solve coarse system based on current saturation
- Assemble fine-scale fluxes
- Advance fine-scale saturation by timestep

end

We note that in the current implementation we use the *hybrid* formulation (Brezzi and Fortin, 1991) which, though equivalent to the mixed formulation, results in a symmetric positive definite linear system of size equal to the number of grid interfaces. The system (4), by contrast, is symmetric but indefinite.

Drift-flux Wellbore Flow Model. The effects of multiphase flow in wellbores can have a strong impact on reservoir performance. Neglecting slip between phases in the wellbore may lead to under-prediction of the pressure drop as the holdup of the heavier phase is not included in the model. As discussed in the Introduction, the in-situ volume fractions are represented here by the drift-flux formulation using the model parameters determined by Shi *et al*. (2005a). In the numerical experiments presented in this paper, we consider only oil-water flow, and thus present details for the oil-water drift-flux model. The gas-liquid and three-phase cases are similar; refer to Shi *et al.* (2005a,b) for further details.

We denote the average oil and water velocities in the wellbore by V_o and V_w and the in-situ volume fractions of the two phases by α_o and α_w, with $\alpha_o + \alpha_w = 1$. The oil and water superficial velocities (V_{so} and V_{sw}) are given by $V_{so}=\alpha_o V_o$ and $V_{sw}=\alpha_w V_w$, respectively. The mixture velocity V_m is then given as the sum of the oil and water superficial velocities:

$$V_m = V_{so} + V_{sw} = \alpha_o V_o + \alpha_w V_w. \quad \text{.....(11)}$$

As in the gas-liquid drift-flux model, the relationship between the phase velocities in the oil-water model is given by (Hassan and Kabir, 1999)

$$V_o = C_0 V_m + V_d, \quad \text{.....(12)}$$

where C_0 is a parameter depending on the phase and velocity profiles over the pipe cross section and V_d is the drift velocity due to buoyancy effects. In general both C_0 and V_d depend on α_o and other quantities. For flow in inclined pipes, the drift velocity in Eq. (12) is scaled by a multiplier $m(\theta)$ where θ is the angle of deviation from the vertical, such that

$$V_{d,\theta} = m(\theta) V_d.$$

Based on the large-diameter experiments of Oddie *et al.* (2003), Shi *et al.* (2005a) suggested the use of $C_0 = 1$ and $V_d = 1.53 V_c (1 - \alpha_o)$. Here V_c is the characteristic velocity of an oil droplet rising in stagnant water and is given by

$$V_c = \left(\frac{\sigma_{ow} g (\rho_w - \rho_o)}{\rho_w^2} \right)^{1/4}, \quad \text{.....(13)}$$

where σ_{ow} is the oil/water surface tension, g is the gravitational acceleration and ρ_o, ρ_w are the phase densities. The corresponding deviation multiplier was determined to be

$$m(\theta) = 1.07 \cos(\theta) + 3.23 \sin(2\theta) - 2.32 \sin(3\theta). \quad \text{.....(14)}$$

Assuming incompressibility, the governing equation for oil-water flow in a wellbore can be expressed by writing the mass balance for oil

$$\frac{\partial \alpha_o}{\partial t} - \frac{\partial V_{so}}{\partial x} = q_o. \quad \text{.....(15)}$$

Here x is the coordinate along the wellbore and q_o is the inflow to the well from the reservoir. This term acts to couple the reservoir and wellbore flow equations. The inflow q_o depends on the reservoir and wellbore pressures and the oil mobility in the near-well reservoir region. We next describe the determination of the pressure profile in the wellbore.

Pressure Drop Calculations. The pressure drop along the wellbore depends on the in-situ phase fractions and can be expressed as (Ouyang *et al.*, 1998):

$$\frac{\partial p}{\partial x} = \rho_m g \sin(\theta) + \frac{2 f_{tp} \rho_m V_m^2}{D} + \frac{2 q_m \rho_m V_m}{A}. \quad \text{.....(16)}$$

Here D and A are the inner cross-sectional diameter and area, ρ_m is the mixture density, q_m is the mixture reservoir inflow and f_{tp} is the Fanning friction suggested by Haaland (1981), which depends on the Reynolds number and the absolute roughness of the pipe. All mixture quantities are computed as the weighted average of the individual phase quantities with respect to the in-situ phase fractions as in Eq. (11). The three terms in Eq. (16) are due to hydrostatic, friction and acceleration effects respectively.

Linkage of Reservoir and Wellbore Flow Models

Gridding around the Well. Our focus here is on capturing near-well heterogeneities down to the scale of the wellbore. Therefore, as a starting point we consider a fine grid that completely resolves the wellbore trajectory, including the wellbore segments which are modeled as cylinders. Based on this fine grid we perform a partitioning into a coarse grid. Figure 2 shows an example of such a grid, where the coarse blocks are indicated by coloring. The special choice here is that the well segments are also treated as individual "blocks" in the coarse grid. Figure 3 shows a cross section of two possible coarse grids around a well. Note that in the coarse grid to the right, the well segment (itself being a coarse block) is completely encapsulated in the surrounding coarse block, and thus the coarse grid here differs considerably from a standard simulation grid. There are two motives that justify this choice. First, it facilitates an easy coupling with the wellbore flow model, and second, it eliminates the need for well indices. The well index is, however, in a sense incorporated into the basis function corresponding to the interface between the segment and the surrounding block.

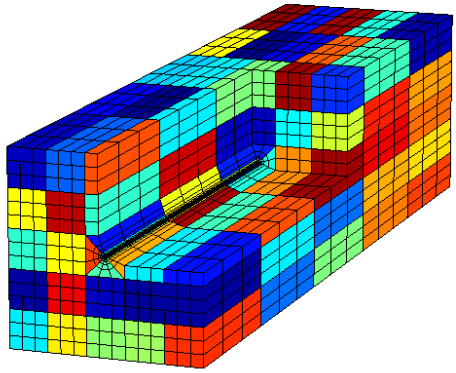

Figure 2: Cutaway view of the fine and coarse grids. Fine grid is radial around the well. Coarse blocks indicated by coloring.

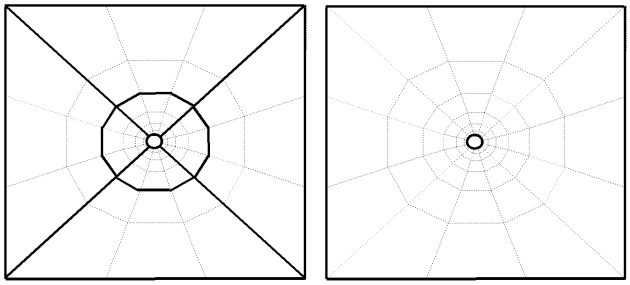

Figure 3: Cross sections of two coarse grids over the same fine grid. Including the well segment the grid on the left contains nine coarse blocks and the grid on the right contains two blocks.

Sequential Splitting of the Equations. Using the MsMFEM requires solving the reservoir equations (1)-(2) sequentially. Thus, we need a similar splitting for the wellbore flow (drift-flux) model.

Pressure Equations. The pressure drop relations of Eq. (16) are discretized and coupled to the system (4) holding the current phase fractions fixed. The non-linearity in (16) is here treated by a simple linearization such that a fixed-point iteration is required to obtain an initial pressure profile. This approach leads to fast convergence for the numerical examples included in this paper, but we expect that Newton iterations would be more appropriate for pressure boundary conditions, for which the current method converges quite slowly.

We also remark that we treat compressibility and gravity in the MsMFEM only at the coarse level. This compressibility treatment is justified by the fact that we here consider nearly incompressible flow. For highly compressible systems special care must be taken; see Lunati and Jenny (2006) for the treatment of such cases within the multiscale finite volume context. We note further that gravitational effects are often important (if not dominant) in the wellbore for vertical or deviated wells. This can be the case even if gravitational effects in the reservoir are of secondary impact. Through treating the well segments as individual coarse blocks, these effects are taken into account.

Saturation/Holdup Equations. Because the MsMFEM provides a fine-scale velocity field, the saturation equation (2) requires a fast solver. However, an explicit solver is not appropriate in this setting due to the strong timestep restrictions caused by the small grid cells around the wellbore. Here we use an implicit upstream finite volume method (Natvig and Lie, 2006) followed by an explicit step to account for gravitational effects. The implicit method is based on an optimal ordering of the cells such that the Newton iteration can be done in sequence for each individual cell (or small clusters of cells), rather than on the whole system.

For calculation of holdup, we employ the following implicit finite difference approximation to Eq. (15):

$$\frac{\alpha_o^{n+1}-\alpha_o^n}{\Delta t}-\frac{V_{so,in}^{n+1}-V_{so,out}^{n+1}}{L}=q_o\,, \quad \text{.....(17)}$$

where Δt is the timestep, L is the segment length, and $V_{so,in}^{n+1}$, $V_{so,out}^{n+1}$ are the inflow and outflow superficial velocities along the segment. Using an upstream weighting (with respect to oil velocity), and assuming oil can flow only from the reservoir into the segment (and not the other way around), we first advance the reservoir saturation to obtain q_o, and then solve (17) to obtain α_o.

We note here that the formulation outlined above represents in some sense a prototype implementation. Several enhancements will be required in order to develop a model that is applicable and robust for more general flow scenarios such as three-phase flow. These include a more general treatment of compressibility, the handling of dissolved gas, and increased implicitness in the formulation.

Numerical Results

Homogenous Model with a Vertical Well. The purpose of this example is to validate the current implementation against GPRS, a general purpose research simulator developed in the Department of Energy Resources Engineering, Stanford University (the initial GPRS implementation was by Cao, 2002). We compare both the mimetic method on the fine grid and the MsMFEM on the coarse grid to the GPRS results. The model is a $4200\,\text{ft}\times 4200\,\text{ft}\times 600\,\text{ft}$ homogenous reservoir (k=200 md, ϕ=0.3) with a vertical well situated in the center. The wellbore has an inner diameter of 1/6 ft and the roughness is set to 0.001 ft. The well penetrates the entire reservoir and is modeled with 12 segments (see Figure 4). The reservoir has an initial water saturation of 0.5 everywhere. We set water and oil relative permeabilities as $k_{rw}=S^2$ and $k_{ro}=(1\text{-}S)^2$, viscosities as $\mu_w=\mu_o=1$, and densities as ρ_w=64.8 $\text{lb}_\text{m}/\text{ft}^3$ and ρ_o=49.2 $\text{lb}_\text{m}/\text{ft}^3$. The oil and water compressibilities are both set to 3×10^{-6} psi^{-1}. The reservoir is sealed on all boundaries.

The fine grid (Figure 4) for this case consists of 7056 cells, while the coarse grid contains 284 blocks. In addition, the 12 segments are included in both the fine and coarse grid. Each coarse block either consists of $3\times3\times2$ Cartesian cells or, if it encapsulates a well segment, $13\times12\times2$ radial cells. The GPRS grid contains 588 blocks. We run one simulation with prescribed total rate of 1600 STB/d and one with total rate 20000 STB/d. For both the mimetic method and the MsMFEM, the prescribed rate is incorporated as a flux boundary condition on the top face of the top segment.

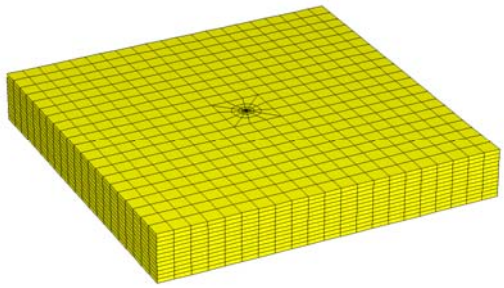

Figure 4: Fine grid with radial resolution around the well in the center of the model.

We first consider the case with a production rate of 1600 STB/d. Results for wellbore pressure after one day of production are shown in Figure 5, while those for in-situ oil fraction (α_o) are shown in Figure 6. For both sets of results, it is apparent that the fine-grid mimetic method and the coarse-grid MsMFEM solutions are in close agreement with the reference GPRS results. The wellbore pressure in this case is almost linear, which is due to the fact that hydrostatic effects dominate. The low velocity, however, results in considerable holdup of water as seen in Figure 6. For the high flow rate case, the pressure drop is considerably larger (Figure 7) due to friction (and to some extent acceleration). Here water and oil flow at close to equal rates as seen in Figure 8. For these simulations we again observe close agreement between MsMFEM, the fine-scale mimetic method, and GPRS. The

agreement evident in Figures 5-8 suggests that both the mimetic and MsMFEM implementations (including the linkage of the reservoir to the wellbore) are correct.

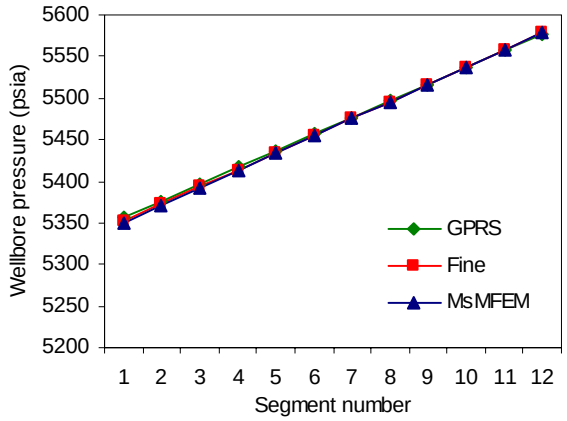

Figure 5: Wellbore pressure profiles for low flow rate case (1600 STB/d).

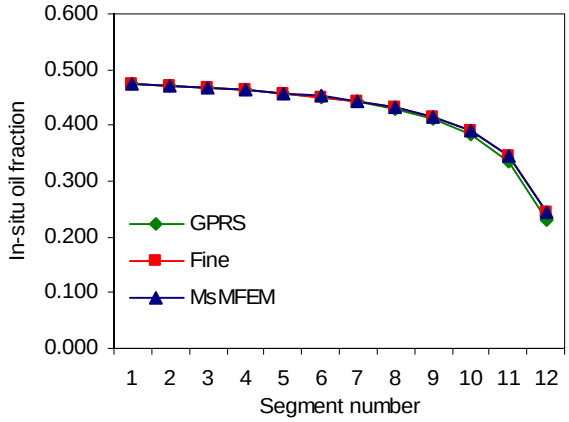

Figure 6: Wellbore in-situ oil fraction for low flow rate case (1600 STB/d).

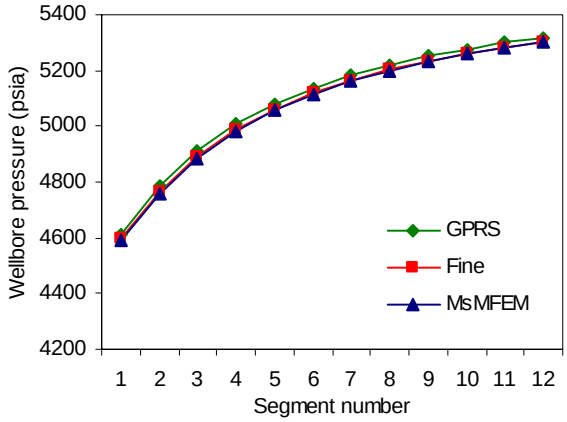

Figure 7: Wellbore pressure profiles for high flow rate case (20000 STB/d).

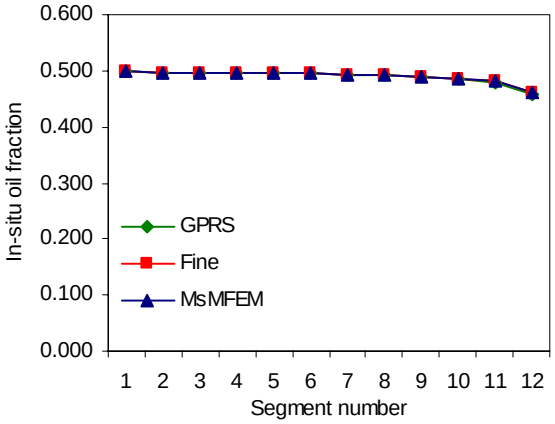

Figure 8: Wellbore in-situ oil fraction for high flow rate case (20000 STB/d).

Heterogeneous Model with an Inclined Well. In this example we consider a larger heterogeneous model with permeability sampled from the tenth SPE comparative solution project (Christie and Blunt, 2001), with additional variability introduced in the near-well region. The model depicted in Figure 9 has a thickness of about 600 ft and extends $5000\,\text{ft} \times 3500\,\text{ft}$ in the horizontal directions. The well configuration (Figure 10) consists of one vertical injection well and one long production well with angle of inclination θ varying from 70^{o} to 80^{o}. The wellbore is modeled using 62 segments. The inner wellbore diameter is 1/3 ft and the roughness is again 0.001 ft. The fine grid has about 85000 cells and the coarse grid consists of $17 \times 24 \times 7$ (for a total of 2856) blocks plus the 62 segments. We consider incompressible flow, quadratic relative permeabilities (as above) and viscosities μ_w= 0.3 cp and μ_o= 3 cp. Densities are as in the previous example. The reservoir is initially filled with oil and water is injected at a constant rate. Two flow rates (with balanced injection and total production) are again considered: 4000 STB/d and 60000 STB/d. Results are presented at 0.12 pore volume injected.

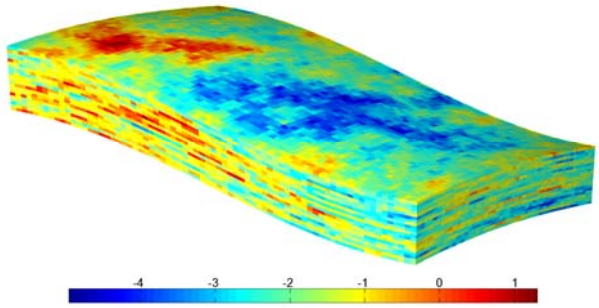

Figure 9: Heterogeneous permeability field (logarithm of permeability displayed).

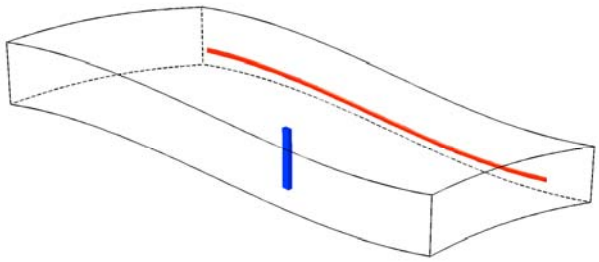

Figure 10: Vertical injection well and inclined production well.

Figure 11 displays the wellbore pressures for the two flow rates. For both cases, the pressure drop given by MsMFEM matches the fine-scale solution essentially exactly, but an error in absolute pressure, although not excessive, is apparent for the high flow rate case. In fact, the error in pressure is close to proportional to the total reservoir pressure drop. The corresponding curves for in-situ oil fraction agree closely (Figure 12). We note that the abrupt behavior of the in-situ oil fraction curve towards the toe of the well (for the 4000 STB/d case) occurs because this part of the well penetrates a low permeability region. As a result the wellbore mixture velocity here is very small, and thus small amounts of water may cause large holdup. For this case, there is no water breakthrough at the last segment, so α_o=1 there. A few segments further towards the heel, however, the water inflow results in a large water holdup (and thus the abrupt drop in α_o). For the high flow rate case (60000 STB/d) this behavior is not observed.

To gauge the variation in accuracy of the MsMFEM solution with increased coarsening, we now consider four different coarse grids for this case. The finest grid is $17\times24\times21$ with an additional partitioning in the near-well region as in Figure 3 (left), giving a total of about 12000 blocks. The coarser grids contain $17\times24\times7$, $10\times12\times4$ and $5\times5\times4$ blocks, respectively. In Figure 13, the pressure profiles for the 4000 STB/d case are shown. The profiles for the three finest grids are fairly close, while the coarsest grid shows some discrepancies (although the pressure drop along the well continues to match the fine-grid solution). The corresponding in-situ oil fraction is depicted in Figure 14, where all the grids produce reasonable results, though again degradation in accuracy with increased coarsening is observed. For the high flow rate case (not shown), trends similar to those in Figures 13 and 14 are observed. These results indicate that, although the accuracy does degrade with increased coarsening (as would be expected), the method continues to provide sensible results even with very coarse grids.

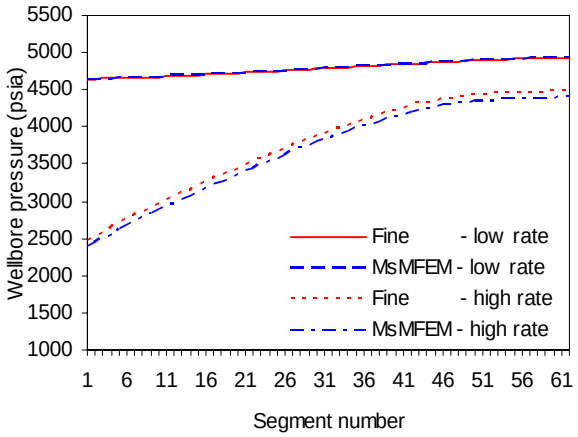

Figure 11: Wellbore pressure profiles for high (60000 STB/d) and low (4000 STB/d) flow rate cases.

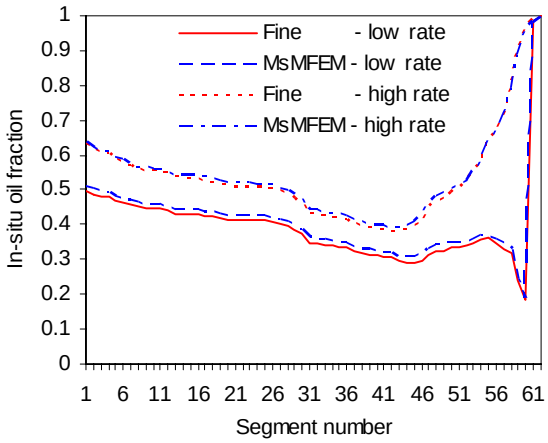

Figure 12: Wellbore in-situ oil fraction for high and low flow rate cases.

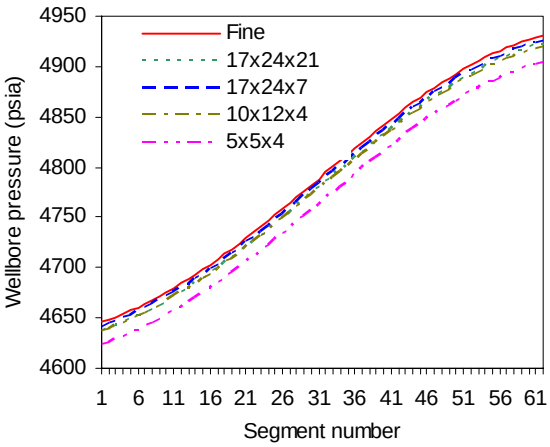

Figure 13: Wellbore pressure profiles for low flow rate case with varying degrees of coarsening.

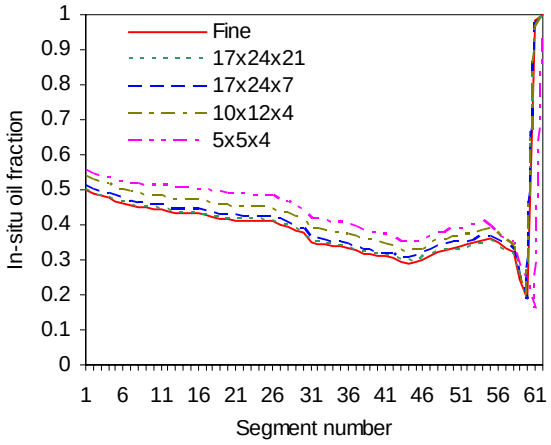

Figure 14: Wellbore in-situ oil fraction for low flow rate case with varying degrees of coarsening.

Concluding Remarks

In this paper we have presented a coupled two-phase wellbore-reservoir flow model that is based on a multiscale mixed finite element method for reservoir flow linked to an oil-water drift-flux model for wellbore flow. By resolving the wellbore trajectory in the fine grid, the methodology successfully incorporates near-well heterogeneity down to the scale of the wellbore and avoids the use of well indices. Through use of multiscale resolution the number of coarse blocks can be kept relatively low, enhancing the efficiency in solving the coupled pressure equations.

The implementation was validated against an existing simulator and we presented numerical simulations involving vertical and deviated wells in a heterogeneous reservoir. The results demonstrate that we have successfully coupled wellbore and reservoir flow models within a multiscale finite element context. The MsMFEM model was shown to provide accurate results on significantly coarsened models in cases with substantial wellbore pressure variation. Future efforts should be directed toward increasing the degree of implicitness of the formulation and extending the procedure to three-phase flow.

Acknowledgements

We are grateful to S. Livescu (Stanford University) for running the comparison simulations in GPRS and to J. Natvig (SINTEF) for providing his code for the discontinuous Galerkin schemes with optimal ordering of elements. This work was funded in part by the Research Council of Norway under grant no. 162606/V30.

Nomenclature

C_0	profile parameter in drift-flux model
g	gravitational acceleration
k, $\mathbf{k}$	absolute permeability, scalar and tensor
k_r	relative permeability
m	deviation multiplier
MFEM	mixed finite element method
MsMFEM	multiscale mixed finite element method
$\mathbf{n}$	normal vector to interface or boundary
p	pressure
q	source term
S	water saturation
t	time
T	cell or block
trace	sum of diagonal entries of matrix
$\mathbf{u}$	Darcy velocity
V, V_s	velocity and superficial velocity along wellbore
$\mathbf{x}$, x	coordinate, in reservoir and along wellbore
α	in-situ wellbore volume fraction
ϕ	porosity
φ	pressure basis function
Γ	interface between cells or blocks
λ	total mobility
μ	viscosity
θ	angle of deviation from vertical
ρ	density
$\boldsymbol{\psi}$	flux basis function
Ω	computational domain

Subscripts

d	drift
m	mixture
i, j	index to cell or block
ij	referring to interface between cells/blocks i and j
o	oil
w	water

References

Aarnes, J. E. 2004. On the use of a mixed multiscale finite element method for greater flexibility and increased speed or improved accuracy in reservoir simulation. *Multi. Mod. Sim.* **2**(3): 421-439.

Aarnes, J. E., Krogstad, S. and Lie, K.-A. 2006a. A hierarchical multiscale method for two-phase flow based upon mixed finite elements and nonuniform coarse grids, *Multi. Mod. Sim.* **5**(2): 337-363.

Aarnes, J. E., Krogstad, S. and Lie, K.-A. 2006b. Multiscale mixed/mimetic finite-element methods on corner-point grids. Submitted to *Comp. Geosci.*

Arbogast, T. 2000. Numerical subgrid upscaling of two-phase flow in porous media. Numerical Treatment of Multiphase Flows in Porous Media, eds. Z. Chen et al., *Lecture Notes in Physics*, **552**: 35-49.

Brezzi, F. and Fortin, M. 1991. *Mixed and hybrid finite element methods.* Computational Mathematics, Springer-Verlag, New-York.

Brezzi, F., Lipnikov, K. and Shashkov, M. 2005a. Convergence of mimetic finite difference methods for diffusion problems on polyhedral meshes. *SIAM J. Num. Anal.* **43**: 1872-1895.

Brezzi, F., Lipnikov, K. and Simoncini, V. 2005b. A family of mimetic finite difference methods on polygonal and polyhedral meshes. *Math. Models Methods Appl. Sci.* **15**: 1533-1553.

Cao, H. 2002. *Development of techniques for general purpose simulators*. PhD thesis, Stanford University.

Chen, Z. and Hou, T. 2003. A mixed multiscale finite element method for elliptic problems with oscillating coefficients. *Math. Comp.* **72**: 541-576.

Chen, Z. and Yue, X. 2003. Numerical homogenization of well singularities in the flow transport through heterogeneous porous media. *Multi. Mod. Sim.* **1**: 260-303.

Christie, M. A. and Blunt M. J. 2001. Tenth SPE comparative solution project: a comparison of upscaling techniques. *SPEREE* **4**(4): 308-317.

Haaland, S. E. 1981. Simple and explicit formula for the friction factor in turbulent pipe flow including natural gas pipelines. IFAG B-131, Technical Report, Division of Aero- and Gas Dynamics, The Norwegian Institute of Technology, Norway.

Hasan, A. R. and Kabir, C. S. 1999. A simplified model for oil/water flow in vertical and deviated wellbores. *SPEPF* (1): 56-62.

Holmes, J. A. 1977. Description of the drift flux model in the LOCA Code RELAP-UK. I. Mech. E. paper 206/77, Proceedings of the Conference on Heat and Fluid Flow in Water Reactor Safety, Manchester, UK.

Holmes, J. A., Barkve, T. and Lund, O. 1998. Application of a multisegment well model to simulate flow in advanced wells. SPE paper 50646 presented at the European Petroleum Conference, The Hague, 20-22 October.

Hou, T. and Wu, X.-H. 1997. A multiscale finite element method for elliptic problems in composite materials and porous media. *J. Comput. Phys.* **134:** 169-189.

Hyman, J., Morel, J., Shashkov, M. and Steinberg, S. 2002. Mimetic finite difference methods for diffusion equations. *Comp. Geosci.* **6**: 333-352.

Hyman, J., Shashkov, M. and Steinberg, S. 1997. The numerical solution of diffusion problems in strongly heterogeneous non-isotropic materials. *J. Comput. Phys.* **204**: 633-665.

Jenny, P., Lee, S. H. and Tchelepi, H. 2003. Multi-scale finite-volume method for elliptic problems in subsurface flow simulation. *J. Comput. Phys.* **187**(1): 47-67.

Jenny, P., Lee, S. H. and Tchelepi, H. 2004. Adaptive multiscale finite-volume method for multiphase flow transport in porous media. *Multi. Mod. Sim.* **3**(1): 50-64.

Lunati, I. and Jenny, P. 2006. Multiscale finite-volume method for compressible multiphase flow in porous media. *J. Comput. Phys.* **216**: 616-636.

Natvig, J. R. and Lie, K.-A. 2006. Fast computation of multiphase flow in porous media by implicit discontinuous Galerkin schemes with optimal ordering of elements. Submitted. url: www.math.sintef.no/geoscale.

Oddie, G., Shi, H., Durlofsky, L. J., Aziz, K., Pfeffer, B. and Holmes, J. A. 2003. Experimental study of two and three phase flows in large diameter inclined pipes. *Int. J. Multiphase Flow* **29**: 527-558.

Ouyang, L. B., Arbabi, S. and Aziz, K. 1998. A single-phase wellbore-flow model for horizontal, vertical, and slanted wells. *SPEJ* **3**: 124-133.

Shi, H., Holmes, J. A., Diaz, L. R., Durlofsky, L. J. and Aziz, K. 2005b. Drift-flux parameters for three-phase steady-state flow in wellbores. *SPEJ* **10** (2): 130-137.

Shi, H., Holmes, J. A., Durlofsky, L. J., Aziz, K., Diaz, L. R., Alkaya, B. and Oddie, G. 2005a. Drift-flux modeling of two-phase flow in wellbores. *SPEJ* **10** (1): 24-33.

Wolfsteiner, C., Lee, S. H. and Tchelepi, H. A. 2006. Well modeling in the multiscale finite volume method for subsurface flow simulation. *Multi. Mod. Sim.* **5**: 900-917

Zuber, N. and Findlay, J. A. 1965. Average volumetric concentration in two-phase flow systems. *J. Heat Transfer, Trans. ASME* **87**: 453-468.